

## Wide-field-angle behavior of blazed-binary gratings in the resonance domain

Mane-Si Laure Lee, Philippe Lalanne, Jean-Claude Rodier, Edmond Cambril

► **To cite this version:**

Mane-Si Laure Lee, Philippe Lalanne, Jean-Claude Rodier, Edmond Cambril. Wide-field-angle behavior of blazed-binary gratings in the resonance domain. *Optics Letters*, Optical Society of America, 2000, 25 (23), pp.1690-1692. <10.1364/OL.25.001690>. <hal-00877446>

**HAL Id: hal-00877446**

**<https://hal-iogs.archives-ouvertes.fr/hal-00877446>**

Submitted on 28 Oct 2013

**HAL** is a multi-disciplinary open access archive for the deposit and dissemination of scientific research documents, whether they are published or not. The documents may come from teaching and research institutions in France or abroad, or from public or private research centers.

L'archive ouverte pluridisciplinaire **HAL**, est destinée au dépôt et à la diffusion de documents scientifiques de niveau recherche, publiés ou non, émanant des établissements d'enseignement et de recherche français ou étrangers, des laboratoires publics ou privés.

# Wide-field-angle behavior of blazed-binary gratings in the resonance domain

Mane-Si Lauree Lee, Philippe Lalanne, and Jean-Claude Rodier

Laboratoire Charles Fabry de l'Institut d'Optique, Centre National de la Recherche Scientifique, B.P. 147, F-91403 Orsay Cedex, France

Edmond Cambril

Laboratoire de Microstructures et de Microélectronique, Centre National de la Recherche Scientifique, 196 Avenue Henri Ravera, B.P. 107, F-92225 Bagneux, France

Received July 17, 2000

Blazed-binary gratings for which a blazed effect with binary etches is achieved under normal incidence offer first-order diffraction efficiencies larger than those of blazed-échelette gratings in the resonance domain [Opt. Lett. **23**, 1081 (1998)]. We provide further insight into the behavior of blazed-binary gratings and show that they operate efficiently under symmetrical mounting and over a wide field-angle interval. These properties are illustrated with theoretical and experimental results obtained for an  $\approx 1000$ -line/mm grating at 633 nm. © 2000 Optical Society of America

OCIS codes: 050.1970, 050.1950, 050.1380.

Standard blazed-échelette diffractive elements fabricated with single-point laser or electron-beam writers offer highly efficient blazes when the local period is much larger than the wavelength. In the resonance domain (grating periods of the order of a few wavelengths), the performance of these continuous-profile elements deteriorates significantly because of the so-called shadowing effect. This deterioration prevents achievement of highly efficient diffractive elements with high numerical apertures.

Recent experimental evidence<sup>1,2</sup> showed that blazed-binary diffractive elements, a family of diffractive elements composed of subwavelength binary features etched into dielectric materials, do not suffer from the shadowing effect and offer high performance in the resonance domain. Another striking example of high performance is observed for the 990-nm-period grating shown in Fig. 1; under normally incident unpolarized illumination at 633 nm, the measured first-order transmitted efficiencies of this blazed-binary grating are 78% (illumination from glass) and 79% (illumination from air), values that are 21% and 49% higher, respectively, than those achieved theoretically by use of a blazed-échelette grating etched into glass with the same period,  $\Lambda = 990$  nm. The high performance of blazed-binary diffractive elements in the resonance domain is intrinsic to their binary profile; it is due to a waveguiding effect<sup>3</sup> through the subwavelength features and, consequently, to a reduction of the shadowing effect. In this Letter we provide further insight into the unusual behavior of these gratings and show that blazed-binary gratings exhibit high performance under a wide range of angles of incidence, thus making them attractive for operation in compact systems with oblique incident beams.

The principle of operation of blazed-binary diffractive elements relies on the analogy between periodic subwavelength structures and artificial dielectric materials.<sup>4,5</sup> With this analogy, index-gradient diffractive elements that produce a blazed effect in a specified

transmitted diffracted order, in general the first order, are implemented with only binary profiles. The grating shown in Fig. 1 follows this analogy and is an implementation of a one-dimensional (1D) phase function that is linearly varying from 0 to  $2\pi$  within the 990-nm period. For this design the phase function is sampled on a regular bidimensional grid with 330-nm spacing. This sampling results in three pillars per period. The pillar widths are fixed by a calibration curve that relates the phase delay for a given etched depth to the fraction of etched material that is removed, or equivalently to the local effective index. More details can be found in procedure 2 of Ref. 2. The maximum effective index ( $n_{\max}$  in Ref. 2) is 1.77, and the  $\text{TiO}_2$ -film ( $n = 2.3$ ) thickness is  $h = \lambda / (n_{\max} - 1) = 817$  nm. Fabrication of the grating relies on electron-beam writing in a poly(methyl methacrylate) layer, lift-off with a nickel mask, and reactive-ion etching into the  $\text{TiO}_2$  thin film. The slight roughness observed in Fig. 1 at

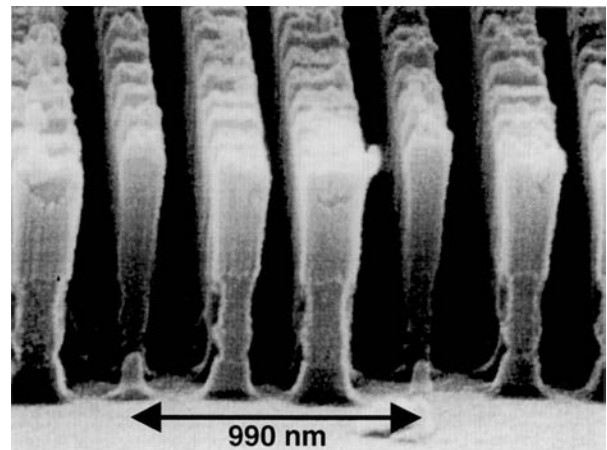


Fig. 1. Scanning electron microscope photograph of a 990-nm-period blazed-binary grating. The center-to-center pillar spacing is 330 nm.

the bottom of the pillars is likely to be due to a technical problem during argon-ion-assisted  $\text{TiO}_2$ -film deposition. The roughness at the top of the pillars is due to the gold layer that was deposited for scanning electron microscope observation. The written grating pattern is a  $208\text{-}\mu\text{m}$ -side square.

The grating is tested with a He-Ne laser beam ( $\lambda = 633\text{ nm}$ ) that is slightly focused with a lens of  $43\text{-mm}$  focal length. Fixing the grating on a rotation stage allows for measurement over a range of angles of incidence. We determine the first-order diffraction efficiency by measuring the power of the first-order diffracted beam and dividing it by the power of the incident beam. The measurements are numerically corrected for Fresnel losses incurred at the rear surface of the glass substrate.

Figure 2 shows the first-order efficiency of the grating shown in Fig. 1, when the grating is illuminated from the substrate with unpolarized light, as a function of angle of incidence  $\theta$  in air. The efficiency is weakly dependent on the polarization. The two experimental curves correspond to conical incidence (the plane of incidence parallel to the grating grooves) and classical incidence (the plane of incidence perpendicular to the grating grooves). Similar behavior is obtained for grating illumination from air. The solid curves are rigorous numerical results obtained with the Fourier modal method.<sup>6</sup> Basically, good agreement between experimental and numerical results is obtained, although we note that, at small angles of incidence, the measured efficiencies are  $\approx 10\%$  lower than the theoretical predictions. This  $10\%$  deviation was already observed in previous work<sup>2</sup> and is attributed to fabrication errors. The conical incidence behavior is similar to that obtained with a standard blazed-*échelette* grating. This behavior is weakly dependent on the incidence angle. More noteworthy is the classical incidence behavior: (1) A plateau with efficiencies greater than  $70\%$  is obtained for angles of incidence in the interval  $[-55^\circ; 8^\circ]$ , and (2) maximum diffraction efficiency is obtained for an oblique incidence of  $\approx -20^\circ$ . We also note two minima of the efficiency at  $\theta \approx -30^\circ$  and  $\theta \approx -10^\circ$ . They are due to a redistribution of the energy into the negative-first reflected and negative-second transmitted orders.

The maximum efficiency (experimentally found to be  $86\%$ ) is achieved for  $\theta \approx -20^\circ$  and incidence angle approximately equal to the Littrow angle,  $|\sin\theta_B| = \lambda/2\Lambda$ . This maximum efficiency in the symmetrical condition is not fortuitous. It was also observed for the  $3\lambda$ -period blazed-binary grating presented in Ref. 2 ( $\theta_B \approx -10^\circ$  in that case). The symmetrical mount is an important geometry for gratings in practice because it allows for high efficiency. For reflection gratings, high diffraction efficiencies at the Littrow angle were already reported for various profiles.<sup>7</sup> The high efficiencies are a direct consequence<sup>7</sup> of the reciprocity theorem and of symmetry. Figure 3 shows the magnetic field distribution inside a 1D  $990\text{-nm}$ -period blazed-binary grating composed of three ridges per period. The grating, which is a 1D version of that shown in Fig. 1, is illuminated from the glass substrate ( $z < 0$ ) by a

TM-polarized light ( $\lambda = 633\text{ nm}$ ) at the symmetrical mount. First, we note that the waveguiding effect<sup>3</sup> also holds at the symmetrical mount. That this is so is clear from the observation of the light confinement in the two upper-right ridges. Second, we note that the Poynting vector, represented by the white arrows in Fig. 3, is nearly vertical over all the grating region. As a consequence, efficient energy flow through the grating is achieved; the theoretical efficiency normalized to the efficiency of all the transmitted orders, a quantity that does not take into account the Fresnel losses, is as high as  $94\%$ . Various simulations have shown that, although the subwavelength ridges behave as waveguides for any oblique incidence, the verticality of the Poynting vector is a unique feature of the symmetrical mount.

Figure 4 shows a comparison of the field-angle dependence of the transmitted first-order efficiency for several grating geometries illuminated under classical mounts from the glass substrate with unpolarized light. The pluses correspond to the experimental results of Fig. 2. The dashed and solid curves are

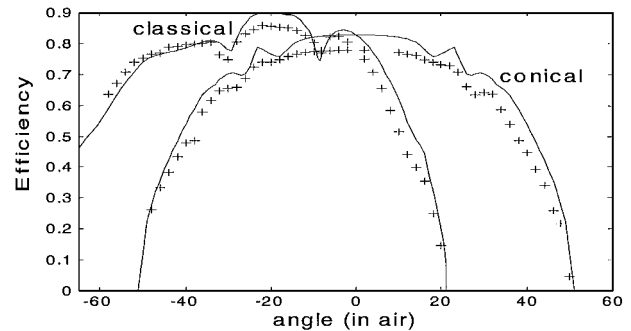


Fig. 2. Transmitted first-order efficiency as a function of angle of incidence (in air). Pluses, experimental results; solid curves, numerical results. The efficiencies are obtained for unpolarized light and for illumination from the glass substrate. The first order is evanescent for incidence angles larger than  $21^\circ$  for the classical diffraction case.

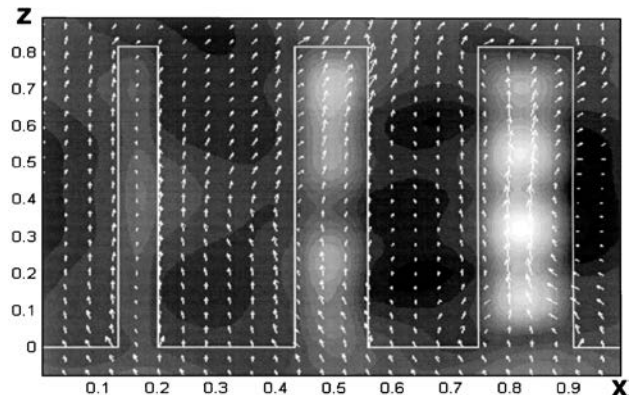


Fig. 3. Distribution of the magnitude of the magnetic field vector inside a  $990\text{-nm}$ -period 1D blazed-binary grating under the symmetrical mount for TM polarization. White areas correspond to large magnitudes. The white arrows represent the average Poynting vectors. The ridge fill factors are  $0.2086$ ,  $0.3745$ , and  $0.4894$ . The corresponding effective indices are  $1.129$ ,  $1.387$ , and  $1.645$ , the same as those of the blazed-binary grating of Fig. 1.

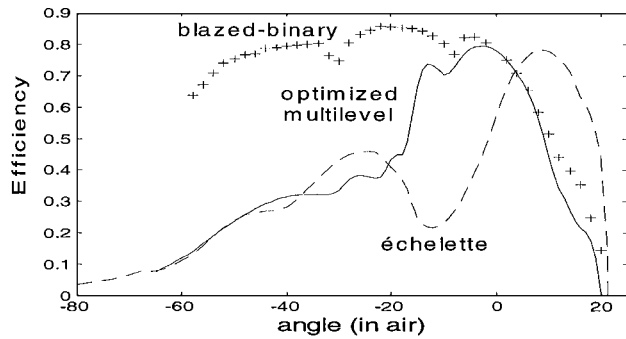


Fig. 4. Field-angle behavior of the transmitted first-order efficiencies for several grating profiles under unpolarized illumination ( $\lambda = 633$  nm) from the glass substrate. Pluses, experimental results of Fig. 2; dashed curve, 990-nm-period *échelette* gratings etched into glass; solid curve, four-level 949-nm-period grating optimized for maximum efficiency at normal incidence (the transition-point locations are given in the first line of Table 2 in Ref. 8).

numerical results. The dashed curve holds for a blazed-*échelette* grating with a 990-nm-period, etched into glass. The solid curve corresponds to a  $1.5\lambda$ -period four-level diffractive grating etched into glass whose transition-point locations are optimized through electromagnetic theory for maximum efficiency under normal incidence.<sup>8</sup> From Fig. 4, it is shown that the diffraction efficiency of the blazed-*échelette* grating is very sensitive to the incidence angle: For  $\theta$  as small as  $-12^\circ$ , the first-order efficiency is only 26%. The optimized multilevel grating offers better performance. At normal incidence, relatively high efficiency (78%) is achieved as a result of parametric optimization. However, the interval  $[-15^\circ; 5^\circ]$  over which the optimized multilevel grating efficiency is greater than 70% is only  $20^\circ$ , as opposed to the  $60^\circ$  interval achieved with the blazed-binary grating. Although parametric optimization makes physical insight into the field-angle behavior of the optimized multilevel grating difficult, we note that, for  $\theta < -20^\circ$ , the performance of the *échelette* grating and that of the optimized multilevel grating are similar. This observation indicates that the field-angle behavior of these two gratings is likely to be dominated

by the same physical phenomena, a shadowing effect<sup>3</sup> and a phase shift that increasingly departs from the ideal  $0-2\pi$  shift as the incidence becomes oblique. Blazed-binary gratings behave in a rather different way from blazed gratings. Their field-angle behavior is driven both by the effective-index dependence on the incident angle and by the waveguiding effect. The latter is effective even for large  $\theta$  values. Consequently, high diffraction efficiencies are achieved over a wide range of angles of incidence. Unlike the optimized multilevel grating, the blazed-binary grating operation does not rely on any electromagnetic refinements of the pillar widths or locations; the sub-wavelength features are directly obtained by physical considerations through effective-medium theory. We believe that this physical base is responsible for the wide-field-angle acceptance of blazed-binary gratings.

In conclusion, this study has revealed that blazed-binary gratings operating in the resonance domain with unpolarized light present nearly maximal efficiencies at the symmetrical mount and offer high efficiencies over a wide field-angle interval. These interesting features make blazed-binary diffractive elements attractive candidates for operation in compact systems with focused beams or oblique incidences.

The authors thank Pierre Chavel and Mike Hutley for fruitful discussions. Laure Lee is grateful to the Délégation Générale de l'Armement for her Ph.D. fellowship. P. Lalanne's e-mail address is philippe.lalanne@iota.u-psud.fr.

## References

1. Ph. Lalanne, S. Astilean, P. Chavel, E. Cambril, and H. Launois, *Opt. Lett.* **23**, 1081 (1998).
2. Ph. Lalanne, S. Astilean, P. Chavel, E. Cambril, and H. Launois, *J. Opt. Soc. Am. A* **16**, 1143 (1999).
3. Ph. Lalanne, *J. Opt. Soc. Am. A* **16**, 2517 (1999).
4. W. Stork, N. Streibl, H. Haidner, and P. Kipfer, *Opt. Lett.* **16**, 1921 (1991).
5. W. M. Farn, *Appl. Opt.* **31**, 4453 (1992).
6. L. Li, *J. Opt. Soc. Am. A* **14**, 2758 (1997).
7. D. Maystre, M. Nevière, and R. Petit, in *Electromagnetic Theory of Gratings*, R. Petit, ed. (Springer-Verlag, Berlin, 1980), Chap. 6, p. 174.
8. E. Noponen, J. Turunen, and A. Vasara, *Appl. Opt.* **31**, 5910 (1992).